Title

Chronic inhalation of e-cigarette vapor containing nicotine disrupts airway barrier function and induces systemic inflammation and multiorgan fibrosis in mice

Journal

AJP Regulatory Integrative and Comparative Physiology, 314(6)

ISSN

0363-6119

Authors

Crotty Alexander, Laura E
Drummond, Christopher A
Hepokoski, Mark
et al.

Publication Date

2018-06-01

DOI

10.1152/ajpregu.00270.2017

Peer reviewed

Title

Chronic Inhalation of E-Cigarette Vapor Containing Nicotine Disrupts Airway Barrier Function and Induces Systemic Inflammation and Multi-Organ Fibrosis in Mice

Short Title

Chronic e-cig use leads to multi-organ fibrosis

Authors

Laura E. Crotty Alexander [1,2,*,#], Christopher A. Drummond [3,*], Mark Hepokoski [1,2], Denzil Mathew [1], Alex Moshensky [1,2], Andrew Willeford [4], Soumita Das [5], Prabhleen Singh [6,7], Zach Yong [1,2], Jasmine H. Lee [8], Kevin Vega [5], Ashley Du [1,2], John Shin [1,2], Christian Javier [1,2], Jiang Tian [9], Joan Heller Brown [4], and Ellen C. Breen [8]

Affiliations

[1] Pulmonary Critical Care (PCC) Section, Department of Medicine, Veterans Affairs San Diego Healthcare System (VASDHS), San Diego, CA

[2] Division of PCC and Sleep Medicine, Department of Medicine, University of California San Diego (UCSD), San Diego, CA

[3] MPI Research Inc., Surgery and Efficacy Department, Mattawan, MI

[4] Department of Pharmacology, UCSD, San Diego, CA

[5] Department of Pathology, UCSD, San Diego, CA

[6] Division of Nephrology and Hypertension, Department of Medicine, UCSD, San Diego, CA

[7] Nephrology Section, Department of Medicine, VASDHS, San Diego, CA

[8] Division of Physiology, Department of Medicine, UCSD, San Diego, CA

[9] Division of Cardiovascular Medicine and Center for Hypertension and Personalized Medicine, Department of Medicine, College of Medicine and Life Sciences, University of Toledo, Toledo, OH

[*] Authors contributed equally

[#] To whom correspondence should be addressed: Laura E. Crotty Alexander, MD, VASDHS 3350 La Jolla Village Dr, MC 111J, San Diego, CA 92161; Phone: 619-438-4207; FAX: 858-546-1754; email: lcrotty@ucsd.edu

Abstract

Background: Electronic (e)-cigarettes theoretically may be safer than conventional tobacco. However, our prior studies demonstrated direct adverse effects of e-cigarette vapor (EV) on airway cells, including decreased viability and function. We hypothesize that repetitive, chronic inhalation of EV will diminish airway barrier function, leading to inflammatory protein release into circulation, creating a systemic inflammatory state, ultimately leading to distant organ injury and dysfunction.

Methods: C57BL/6 and CD-1 mice underwent nose-only EV exposure daily for 3-6 months, followed by cardiorenal physiologic testing. Primary human bronchial epithelial cells were grown at an air-liquid interface and exposed to EV for 15 minutes daily for 3-5 days prior to functional testing.

Results: Daily inhalation of EV increased circulating pro-inflammatory and pro-fibrotic proteins in both C57BL/6 and CD-1 mice: the greatest increases observed were in angiopoietin-1 (31-fold), and EGF (25-fold). Pro-inflammatory responses were recapitulated by daily EV exposures *in vitro* of human airway epithelium, with EV epithelium secreting higher IL-8 in response to infection (227 vs 37 pg/mL, respectively; $p<0.05$). Chronic EV inhalation *in vivo* reduced renal filtration by 20% ($p=0.017$). Fibrosis, assessed by Masson's trichrome and Picrosirius red staining, was increased in EV kidneys (1.86-fold, C57BL/6; 3.2-fold, CD-1; $p<0.05$), heart (2.75-fold, C57BL/6 mice; $p<0.05$) and liver (1.77-fold in CD-1; $p<0.0001$). Gene expression changes demonstrated pro-fibrotic pathway activation. EV inhalation altered cardiovascular function, with decreased heart rate ($p<0.01$), and elevated blood pressure ($p=0.016$).

Conclusions: These data demonstrate that chronic inhalation of EV may lead to increased inflammation, organ damage, and cardiorenal and hepatic disease.

Keywords electronic cigarette, e-cigarette, systemic inflammation, cardiorenal dysfunction, nicotine, fibrosis

Introduction

Electronic cigarettes (e-cigs) became widely available in 2004-2007 (12). They are the newest tobacco products on the market, and work by heating and aerosolizing propylene glycol (PG; 1,2-Propanediol), glycerin (Gly; 1,2,3-Propanetriol) and nicotine. The product inhaled is commonly referred to as e-cig vapor (EV). EV has components in common with cigarette smoke, chief among these nicotine, which can directly cause endothelial dysfunction (56). Some EV also contains acrolein, formaldehyde and nitrosamines, which are also commonly found in cigarette smoke. This commonality raises the concern of shared toxicities between cigarettes and e-cigs (17, 19). The finding that low-tar and smokeless tobacco products may be linked to systemic inflammation and increased cardiovascular disease, further suggests that some of the components of tobacco do not need to undergo combustion in order to be damaging to human health (9, 58). While the lungs are one of the primary sites of ill effects of cigarette smoke (emphysema and lung cancer), tobacco smoke has significant effects on many other organs, including kidneys, heart, brain and gastrointestinal tract, via induction of endothelial damage and systemic inflammation (2, 56, 60).

Many human e-cig users pick up the vaping habit as an attempt to help them quit smoking, however some studies and meta analyses to date suggest that e-cig use reinforces the nicotine addiction and decreases the odds of quitting (25, 39). Our own work has demonstrated that chronic inhalation of EV leads to activation of classic nicotine addiction pathways in the central nervous system (1), which suggests that e-cig users will likely continue using these nicotine delivery devices for years to come. Clinical signals of adverse effects on human health due to long-term use by e-cig users, such as emphysema, cardiovascular disease, and renal dysfunction,

may not, however, be evident for 20-50 years or until they are exacerbated by pathophysiological challenges.

One mechanism by which chronic inhalation of chemicals causes disease is through disruption of the airway epithelial barrier (13, 18, 59, 68). Normal airways have a solid barrier facilitated through the existence of tight-junctions between epithelial cells. Isolated cases of eosinophilic pneumonia (76), lipoid pneumonia (54), acute lung injury and acute respiratory distress syndrome (ARDS; personal communication with Jennifer McCallister, OSU) have been reported in e-cig users, demonstrating that short-term exposure to EV may lead to acute epithelial damage and pro-inflammatory responses within the lungs. We hypothesized that chronic EV inhalation would alter the permeability of epithelial surfaces and increase exposure of parenchymal cells to EV components, leading to damage and inflammation, that promote acute and chronic diseases by recurrent inflammatory signaling driving a systemic pro-inflammatory state.

Our prior studies with EV utilized established *in vitro* models, and demonstrated negative effects on antimicrobial function of lung cells - alveolar macrophages, epithelial cells, and neutrophils (32). Other groups have also found adverse effects on airway cells *in vitro* (79), lung function *in vivo* (51), and increased susceptibility to infection *in vivo* (75). In our lab, we also found significant cell death (cytotoxicity) of EV on all mammalian cell lines evaluated (32). Cell death commonly activates inflammatory pathways (and vice versa) and can produce tissue changes leading to pathology. Finally, we have published that EV exposure *in vitro* can induce double-stranded DNA breaks, a serious effect that can lead to malignant conversion (81).

In the current studies, we explored the hypothesis that exposure to the most common components of EV (PG, Gly, and nicotine) alters barrier function of airway epithelium, leading to release of inflammatory proteins into the systemic circulation. Using our *in vivo* animal model of chronic EV inhalation (32), we assayed serum for evidence of pro-inflammatory effects of EV inhalation, and organs for downstream effects of these pro-inflammatory signals. We specifically evaluated cardiorenal function, as it is known that inhalation of combustible cigarette smoke is detrimental to both cardiac and renal function (30, 63, 74). One group recently published adverse effects of intraperitoneal injection of e-liquid daily for one month on rat kidney function (28). We sought to confirm these findings using a physiologic exposure to EV, in which e-liquid is placed into a tank, attached to a battery, and the e-liquid is heated and vaporized, producing EV which is inhaled through our nose-only system into the airways. The reason for using this more complex type of exposure is that heating and vaporization of e-liquid alters the chemical composition, and can create toxins such as formaldehyde and acrolein; these toxins may cause adverse effects directly on airway and endothelial cells which the other components of EV do not (34, 72, 77).

The following *in vivo* and *in vitro* studies were designed and undertaken to evaluate whether e-cig use leads to inflammation. We present here the effects of daily, chronic inhalation of EV containing nicotine on airway permeability, airway inflammatory response to bacterial infection, the systemic inflammatory milieu, downstream organ function and tissue fibrosis. Informing e-cig users, physicians, businesses and policy makers of the potential risks of these new devices may lead to the production of safer devices, new policies to limit access to adults, and safer use patterns by the vaping community – and thus decreased adverse effects on human health overall.

Materials and Methods

E-cigarettes

E-liquid consisting of 50% propylene glycol (PG), 50% glycerin (Gly; also referred to as vegetable glycerin, VG), and 24 mg/mL nicotine was used, as it was a common solution used by the general population in 2014, at the time of study design. All e-liquids were mixed in the lab after purchase from a popular online vendor (Xtreme Vaping). E-liquid was placed in a standard tank (1.8 Ohm) and was attached to a rechargeable lithium ion battery (3.4 V). All e-cig components were purchased from commercial vendors (FastTech, Vapor Authority, and Xtreme Vaping), to maintain relevance to human e-cig users. All exposures were designed to model firsthand EV exposure, with animals and human cells exposed to EV generated from devices used by actual e-cig users (Figure 1A), and generated with the same pneumatic pressure and puff topography as human e-cig vapers.

Primary human bronchial epithelial cell permeability assay

Primary normal human bronchial epithelial cells (NHBEs) were purchased from Lonza (donors have no reported history of smoking or known lung conditions). The cells were grown according to the manufacturer's established protocols as mentioned previously (52). In brief, the cells were resuspended in growth media (Lonza) and seeded onto cell culture inserts (0.4 μm pore size; Costar), coated with type I rat tail collagen (BD Biosciences). Cells were maintained in B-ALI differentiation media (Lonza) with inducers for 3 weeks in the basal chamber for differentiation into mucociliary cells. Trans-epithelial electrical resistance (TEER) was measured using the Voltohmeter on days 14 and 21, and demonstrated epithelial confluency via increasing electrical

transmittance in all wells. When the TEER values reached a plateau, starting on day 21, NHBE cells were transferred to an exposure chamber and EV or Air was introduced for 15 minutes daily for 2-5 days. Each EV breath (50 mL) was produced by pneumatic activation of the e-cig via a 60 mL syringe (Figure 1B), with exhalation of the EV onto the apical surface of the NHBE cells, followed by 2 air breaths (50 mL apiece), to mimic the act of breathing. Because EV leaves a greasy residue on exposed surfaces, after exposure, transwells were gently transferred to new wells containing fresh media (380 µL) at the basal interface, and were placed back at 37°C with 5% CO_2. NHBE barrier function, and specifically permeability due to interruptions in the junctional complex, was evaluated with and without infection with *Pseudomonas aeruginosa* (PSA; $1x10^6$ CFU/well in 50 µL) PAO1 (16), by application of FITC-dextran, molecular weight 3-5,000 (Sigma) to the apical surface for 15 minutes, followed by transfer of 50 µL from the lower transwell chamber to a flat-bottom 96-well plate. The amount of paracellular permeability was measured using a fluorescence plate reader with excitation of 490 nm and emission at 520 nm. NHBE cells were either kept uninfected or were infected with PSA PAO1 ($1x10^6$ CFU/well in 50 µL) (5). After 2 hours of infection, basolateral supernatant was collected. NHBE cells were harvested either with RLT buffer (Qiagen) or with RIPA buffer and stored at -80°C for RNA and protein studies.

ELISA and Western Blot

The supernatants collected from NHBE cells were measured for IL-8/LIX using the Human IL-8/CXCL8 Quantikine ELISA Kit (R&D systems) following the manufacturer supplied protocol. For Western Blots, cell lysates were prepared from NHBE cells with ice-cold RIPA buffer containing protease inhibitor (Roche) and phosphatase inhibitor (Sigma) cocktails. An equal

amount of protein (50 μg) was loaded in each lane of 8% SDS-PAGE and transferred onto nitrocellulose membrane (Bio-Rad). The membrane was blocked in 5% non-fat milk in TBST (Tris-buffered saline with 0.05% Tween-20), incubated with the tight junction protein antibody for zona occludins (ZO1) (Proteintech; 1:1000) and tubulin (Proteintech; 1:10,000) in 5% milk-TBST for incubation overnight at 4°C. ZO1 was detected at a molecular weight of 195 kD, while tubulin was detected at a molecular weight of 55 kD. After imaging, blots were opened in ImageJ, converted to 8-bit files, background removed via adjustment of the threshold to Huang, and the integrated density of each band was measured.

Animals

Six to eight week-old female C57BL/6 and CD-1 (ICR) mice were purchased from Harlan (Envigo). Inbred C57BL/6 mice are known to be susceptible to emphysema and oxidative stress (29), while outbred CD-1 mice are resistant (14). Mice were acclimated to the individual, soft mesh restraints (SciReq) for 30 min daily for 2 days. Mice were then exposed to EV daily, for 5 days per week, for 3-6 months, using the nose-only InExpose system (SciReq) as we previously described (32), using a flow rate of 2 L/minute and exposure time of 4 seconds of EV every 20 seconds for 60 minutes daily (7). Because C57BL/6 mice are more susceptible to pathologic effects of smoke inhalation (emphysema), and more susceptible to disease in general, the duration of their chronic EV exposure was set at 3 months, while the hardy, emphysema resistant CD-1 strain was exposed to EV for 6 months. Mice in the air control group were placed in the same restraints, but inhaled room air only. Cheek bleeds were performed 30 min post-exposure, and serum cotinine concentration determined via ELISA (Calbiotech). Serum cotinine levels in C57BL/6 mice were 269 ng/mL +/- 15.6, and in CD-1 mice were 288 ng/mL +/- 39, post-EV

exposure for 60 minutes. C57BL/6 mice were exposed to EV or Air daily for 3 months. CD-1 mice were exposed to EV or Air daily for 6 months. All mice were placed in pre-warmed cages for 30 minutes to recover after restraint. The last exposure was done the day of harvest, with mice being placed on a warming pad for heart rate and blood pressure measurements (15-30min post-exposure), followed by application of anesthesia, terminal intracardiac bleed and organ harvest. Animal experiments were conducted in accordance with the National Institutes of Health, Guide for the Care and Use of Laboratory Animals under protocols approved by the Institutional Animal Care and Use Committees at the University of California San Diego and the VA San Diego Healthcare System.

Circulating pro-inflammatory cytokines

Blood was placed at 4°C for 15 min, spun at 3,000 rpm for 15 min at 4°C, and plasma stored at -80°C for measurement of total protein (BCA Total Protein Assay Kit; Pierce) and inflammatory cytokines via Mouse XL Cytokine Array (Proteome Profiler by R&D), according to the manufacturer's instructions. In brief, for CD-1 mice, plasma samples were individually checked for protein concentration prior to pooling for proteome array, with equal volumes of plasma from individual mice combined into one sample (n = 6 for both groups). Individual plasma samples from C57BL/6 mice were run (n = 3 for both groups). Proteome films were blinded, scanned, uploaded to imageJ, background removed via threshold adjustment, and pixel density for each pair of cytokine dots quantified. Data is presented as a ratio of EV to Air.

Renal Function

To determine glomerular filtration rate (GFR), the week prior to harvest, mice were exposed to EV or Air for 60min, and allowed to recover for 60 minutes. Mice were placed under inhaled isoflurane anesthesia and FITC-sinistrin (2 µl/g body weight) was injected retro-orbitally with a 30G needle. Subsequently, the anesthetized mouse fully regained consciousness. Tail vein puncture was utilized to collect blood in 10 µL Na-Heparin Minicaps at the following times after injection: 3, 5, 7, 10, 15, 35, 56, and 75 minutes. Samples were analyzed for FITC-Sinistrin concentration using a NanoDrop 3300.

Cardiac Function

For the week prior to harvest, EV and Air mice underwent heart rate (HR) and blood pressure (BP) monitoring for 30 minutes after EV or Air exposure (n = 6 for all groups). HR and BP were obtained using a CODA Monitor, non-invasive BP system (Kent Scientific) as described previously (23, 42, 43). We concomitantly checked HR via pulse oximeter by PhysioSuite (Kent Scientific).

Renal, cardiac and liver fibrosis evaluation

Mice were anesthetized with ketamine (100 mg/kg) and xylazine (10 mg/mL) and euthanized, by a terminal intracardiac bleed. The right kidney, one lobe of liver and the base of the heart were then immediately dissected and placed in Z-fix at 4°C. After 48 hours all organs were moved to 75% ethanol and submitted to the UCSD histology core for paraffin embedding. Collagen was detected in 5 µm sections first by Masson's trichrome stain. All histology slides underwent quantification of fibrosis by calculating the mean percent fibrotic area in > 30 randomly acquired 20x images using computer aided morphometry performed using a macro in ImageJ as

previously described (23, 31, 42, 43). Collagen deposition was also detected by 5 μm sections on Picrosirius red staining. All histology slides were blinded and underwent quantification under bright field microscopy by calculating a relative area of brightness at a set threshold (157,255), in relation to the area of 6 randomly acquired 10x images, computer aided morphometry performed using an ImageJ macro (https://imagej.nih.gov/ij/docs/examples/stained-sections/index.html). All slides underwent these computer analyses in an identical fashion. Fibrotic area is presented relative to that of air controls.

Quantification of fibrosis markers in renal and cardiac parenchyma

After daily exposure to EV for 5 days per week, for four weeks (1 month), the left kidney and the apex of the heart from both CD-1 and C57BL/6 Air and EV mice were snap frozen and stored at ˉ80°C. 30 mg of frozen left ventricular or renal tissues were homogenized in Trizol and total RNA was isolated using the RNeasy kit (Qiagen), followed immediately by cDNA synthesis using the First Strand cDNA synthesis kit (Qiagen), according to the manufacturer's protocol. 1 μg of total RNA was used for the initial reaction. cDNA was stored at ˉ20°C, and was used for quantitative real-time polymerase chain reaction (qPCR) within 2 weeks.

To quantify extracellular matrix gene expression in murine cardiac and renal tissues, species specific primers were purchased from Qiagen for Collagen 1a1 (Col1a1; PPM03845F), Collagen 3a1 (Col3a1; PPM04784B), Collagen 4a1 (Col4a1; PPM05145A), Matrix metalloprotease 2 (Mmp2; PPM03642C), Integrin beta 1 (Itgb1; PPM03668D), Fibrillin 1 (Fbn; PPM36411E), and Elastin (Eln; PPM36834B), in addition to Glyceraldehyde 3-phosphate dehydrogenase (GAPDH;

PPM02946E) as a control. RT^2 SYBR Green qPCR reaction mix (Qiagen) was used according to the manufacturer's protocol, with an ABI 7500 Fast platform (Life Technologies). Determination of mRNA expression was computed by comparing the relative change in cycle threshold value of the target (ΔCt) from the internal control, GAPDH. Fold change in expression in EV tissues versus air controls was then calculated for each mRNA in each sample using expression = $2^{-\Delta\Delta Ct}$ methodology (36).

Statistical analyses:

Data are presented as means ± Standard Error of the Mean (SEM). Data obtained were analyzed by t-test or by two-way ANOVA, where appropriate. Analyses were conducted using Graph Pad Prism 6 software.

Results

E-cigarette vapor inhalation increased the levels of circulating inflammatory cytokines

We hypothesized that repetitive inhalation of EV leads to stress in or damage to pulmonary epithelial cells, which leads to the release of factors into systemic circulation. In mice inhaling one hour of EV daily, for 5 days per week, we found higher levels of several inflammatory cytokines in the circulation (significance was defined as a 20% change compared with Air control mice), and lower levels as well (Figures 2A-B). Proteins that changed in both strains of mice (*) are of particular interest since these changes were induced by chronic EV inhalation across genetically different backgrounds (Table 1). Proteins from the same family (such as metalloproteases MMP-9 and MMP-2) that had changes in quantity across the two strains are also demarcated (✢). Overall, the finding of changes in expression, production or secretion of

multiple inflammatory protein levels, both increases and decreases, suggests that chronic EV inhalation causes systemic immunomodulation.

To begin to understand where the immunomodulatory signals originate we evaluated the inflammatory state of the lungs. Lungs from CD-1 mice were examined and had normal histopathology (Figure 3A). Within the bronchoalveolar lavage (BAL), dipeptidyl peptidase-4 (DPPIV / CD26) was elevated 1.7-fold in EV mice versus controls (Figure 3B). DPPIV is an enzyme expressed on the surface of cells. It is an intrinsic membrane glycoprotein and has general immune regulation and signal transduction functions. DPPIV has been shown to modulate macrophage M1/M2 polarization (86) and modulate T-cell recruitment to the lungs (49, 71), while inhibition of DPPIV decreases T-cell mediated inflammation (73). DPPIV is thought to play a pathologic role in the development of liver, cardiac, and kidney fibrosis (3, 37, 40, 69).

Nicotine itself has effects on endothelial cell function. The nicotine metabolite cotinine was measured in all mice immediately after the final 60 minute EV or air exposure. C57BL/6 mice exposed to EV had an average plasma cotinine level of 268.8 ng/mL versus 25.6 ng/mL in Air controls, while CD1 female mice exposed to EV had an average of 287.9 ng/mL plasma cotinine, versus 3.1 ng/mL in Air controls.

Short term daily exposure to e-cigarette vapor weakened human airway epithelium barrier function *in vitro*

One mechanism by which chronic inhalation of EV may lead to systemic inflammatory changes is by inducing inflammatory signals at the level of the airways. Exposure of the apical surface of confluent NHBEs to 15 minutes daily of EV for 2 and 5 days led to diminished barrier function with the passage of 48% and 46% more FITC-dextran from the apical surface down through the basal surface, respectively (8,070 vs 4,200 RFI at day 2, and 10,300 vs 5,600 RFI on day 5; $p < 0.01$; Figure 4A). Further increase in permeability was observed in NHBEs following infection with *Pseudomonas aeruginosa*. Secretion of the pro-inflammatory neutrophil chemokine IL-8 by NHBEs increased 6-fold by ELISA quantification, following EV exposure, in the setting of bacterial super-infection ($p < 0.05$; Figure 4B). Tight junction proteins that function to keep the epithelium impermeable were evaluated by Western blot. The level of zona occludens 1 (ZO1) was lower in NHBEs after acute EV exposure ($p = 0.024$), suggesting changes in tight junctions induced by EV exposure (Figure 4C). Decreased tight junction proteins suggest that EV leads to reduced barrier function in the lungs, which in turn can allow greater passage of external factors (antigens and chemicals) into the lung parenchyma and bloodstream.

Chronic exposure to daily e-cigarette vapor induced renal dysfunction and fibrosis in C57BL/6 mice

To determine whether the circulating protein changes demonstrated above are associated with organ dysfunction we first evaluated renal function. Three months of daily EV inhalation induced a 20% reduction in glomerular filtration rate (GFR) in C57BL/6 mice as compared with experimental controls ($p = 0.017$; Figure 5A), as measured by FITC-sinistrin clearance. Using blinded evaluation of Masson's trichrome stained renal parenchyma (Figure 5B), kidneys from EV exposed mice were found to have 87% more collagen in their parenchyma (evidence of renal

fibrosis) than did air controls (1.88-fold increase, $p < 0.05$; Figure 5C). Blinded evaluation of Picrosirius red stained renal parenchyma (Figure 5B) confirmed higher deposition of collagen in EV kidneys compared to air controls (1.62-fold increase, $p = 0.034$; Figure 5D). These data suggest that regular EV inhalation may have pro-fibrotic effects on kidney parenchyma, which could lead to decreased renal function after a relatively short duration of exposure.

Long term e-cigarette exposure in outbred CD-1 mice also induced renal fibrosis

When genetically diverse, and thus hardier, CD-1 mice were exposed to 1 hour daily of EV for 6 months, they also developed renal fibrosis (Figure 6A). By trichrome staining, EV kidney parenchyma had a 3.2-fold increase in fibrosis compared with experimental controls ($p = 0.022$; Figure 6B). By Picrosirius red staining, EV kidney parenchyma had 2.14-fold higher collagen deposition compared to air controls ($p < 0.01$; Figure 6C). These data suggest that chronic inhalation of EV leads to activation of pro-fibrotic pathways systemically, impacting non-pulmonary organs. Changes in pro-fibrotic gene expression were also observed at earlier times (Figure 6D-K). These data add confidence to our findings that fibrosis is stimulated by EV exposure since outbred CD-1 mice are genetically diverse, with higher likelihood of results being translatable to human subjects.

Recent work in our lab has revealed that decreased tissue expression of miR-29b-3p is a mechanism of cardiorenal toxicity and organ fibrosis in chronic kidney disease and in response to combustible cigarette exposure (21, 22, 48). We found molecular evidence of early pro-fibrotic changes in renal tissues of EV exposed mice at 1 month – lower expression of the anti-

fibrotic miRNA miR-29b-3p (Figure 6D) and higher expression of collagen-1 within CD-1 renal parenchyma (Figure 6E). The expression of additional pro-fibrotic factors, Col3a1, Col4a1, Itgb1, and Fbn1, were all significantly increased in renal tissues from e-cigarette exposed animals ($p < 0.05$; Figs. 6F, 6G, 6I, and 6J). Extracellular matrix remodeling factor Mmp2 trended up, but not significantly (Figure 6H). The fibrosis component Eln trended down (Figure 6K). When we completed similar renal studies with our collaborators studying renal fibrosis in a cigarette smoke (CS) inhalation model, we found a similar fibrosis pattern (21). These data suggest that a shared component of EV and CS, such as nicotine, may be the etiologic agent in distant organ injury and fibrosis.

Chronic e-cigarette vapor inhalation induced cardiac fibrosis and altered cardiovascular function

Examination of cardiac tissue revealed a 2.75-fold greater level of fibrosis in hearts from CD-1 mice exposed to EV for 6 months compared with controls ($p < 0.001$; Figures 7A-B). When we examined hearts after only 4 weeks of daily EV exposure, we found increased expression of collagen-3 ($p < 0.05$; Figure 7C), although levels of collagen-1 were not elevated (Figure 7D). These data extend our findings from kidney to heart and thus suggest global pro-fibrotic signaling induced by chronic EV inhalation.

We evaluated cardiovascular function in the C57BL/6 mice exposed to EV for 3 months, and found decreased heart rates (HR), as compared with air controls ($p < 0.01$; Figure 7E). EV mice also tended to have more HR variability (oscillations between consecutive instantaneous HR;

Figure 7F). Systolic blood pressure (SBP) was increased in e-cigarette exposed mice ($p = 0.016$; Figure 7G) and diastolic blood pressure (DBP) trended up ($p = 0.050$; Figure 7H). These data demonstrate effects of daily EV inhalation on cardiac function, including blood pressure and heart rate, which could have a long-term impact on cardiac hypertrophy and function.

Chronic e-cigarette vapor inhalation induced hepatic fibrosis

The finding of multi-organ fibrosis suggests the presence of a circulating pro-fibrotic signal, and the possibility that other susceptible organs may be affected. Livers from CD-1 mice exposed to EV for 6 months were examined in a blinded fashion and consistently shown to have higher levels of fibrosis by collagen staining (Figure 8A-B).

Discussion

E-cigarettes are considered by many to be safer than conventional cigarettes. While this is most likely the case in terms of carcinogenesis (81), conclusions as to their general safety have yet to be made. We present here, for the first time, evidence that chronic e-cigarette use negatively impacts multiple organs in mammals of different genetic backgrounds. Daily inhalation of EV made from PG, Gly and 24 mg/mL nicotine for 3 or 6 months led to fibrosis in heart, kidney, and liver tissues, with concomitant changes in cardiac and renal function. *In vitro* data suggest that toxic components of EV may be disrupting airway epithelium, triggering cells to secrete pro-fibrotic proteins into circulating blood, leading to damage to multiple organs. Although all three organs affected in our studies had a similar pattern of fibrosis, gene expression changes were not identical. Kidney parenchyma had elevations in Col1a1 and Col3a1 at 1 month, while cardiac tissue only had elevation of Col3a1. The regulation of these two collagens in the myocardium is known to be via complex and diverse mechanisms (8, 57). Different organ systems are known to respond to stress and inflammation in different ways, and over different time frames (24). Myofibroblasts arise from stromal cells within each organ and are the primary sources of extracellular matrix protein production. Because myofibroblasts have organ-environment based differences in gene expression, which leads to functional heterogeneity, there are differences in the types of collagen deposited, and the timing thereof, for myofibroblasts from cardiac, renal and hepatic tissues. Although extensive research has been done on fibrosis, there is still much unknown about the multitude of cellular and molecular pathways in fibrosis induction, progression and termination.

Increased levels of circulating inflammatory proteins due to chronic EV exposure

To determine potential pathways through which multi-organ fibrosis is incurred, inflammatory protein profiles were examined using plasma from two mouse strains (C57BL/6 – individual samples; CD-1 – pooled samples). We report here only proteins that were different by 20% or more in EV mice relative to Air controls, as changes of that magnitude have a greater likelihood of potential biologic effects. We focused on changes in circulating inflammatory proteins that occurred in both C57BL/6 and CD-1 strains, as activation of inflammatory pathways in disparate genetic backgrounds are more likely to be associated with the downstream organ damage and fibrosis that was found in our models.

Leukemia Inhibitory Factor (LIF) is a member of the IL-6 cytokine family and is commonly systemically elevated in the setting of inflammation (62). LIF was elevated in the circulation of EV mice, as compared with Air, with a 30.6-fold increase in C57BL/6 mice and a 6.3-fold increase in CD-1 mice (Table 1). LIF is involved with regulation of cell differentiation, proliferation, and survival, via activation of both the JAK/STAT3 and MAPK pathways, which increase the ability of tumor cells to invade. More importantly, LIF is produced by pulmonary cells, including epithelial, smooth muscle and innate immune cells, in response to stressful stimuli, including inhalation of air pollution and endotoxin (47), and is thought to confer protection (78), even in the setting of ARDS. Elevations of circulating LIF in our models suggests that inhalation of EV induces stress on pulmonary cells, leading to production and release of LIF as a protective response. Increased LIF also suggests increased autophagy, which may be an adaptive response to stress or lead to cell death, and LIF is known to increase EGF expression, which experienced a 24.6-fold increase in the plasma of C57BL/6 EV mice, and a

2.1-fold increase in the plasma of CD-1 EV mice (Table 1). Elevated LIF and EGF suggest that EV mice may have systemic increases in cell-proliferation signals.

Angiopoietin 1 (Ang-1) was increased in EV plasma from C57BL/6 and CD-1 mice, compared with experimental controls (27-fold and 1.38-fold higher in EV versus Air, respectively). In human smokers, Ang-1 has been found to be elevated in the blood, before mild, moderate or severe COPD develops (45). This may be due to ongoing vascular remodeling secondary to damage by cigarette smoke inhalation. In a C57BL/6 mouse model of renal injury, Ang-1 was shown to be elevated in the setting of increased fibrosis (84). It has been demonstrated that increased production of Ang-1 by kidney cells can protect against further fibrosis (46, 70). In addition, other data show that the production of Ang-1 can decrease cardiac fibrosis in the setting of myocyte injury (15, 83). Thus, increased release of Ang-1 may also indicate that defensive, protective mechanisms are triggered as a result of renal or cardiac fibrosis in EV mice. Further studies are needed to determine the tissues from which Ang-1 is originating during EV inhalation.

LIX was elevated 1.92-fold (92% increase) in C57BL/6, and 1.24-fold (24% increase) in CD-1 mice. CXCL5 (LIX) is secreted by alveolar epithelial type II cells, and plays a role in recruitment of neutrophils and macrophages into the lungs (4, 35). LIX is known to be elevated in the setting of COPD, smoke exposure, and atherosclerosis (61). Thus, the increase in LIX may contribute to an influx of immune cells into the lung parenchyma, and suggests that further inhalation of EV may lead to disease.

Decreased levels of circulating inflammatory proteins due to chronic EV exposure

MMP-3 has the capacity to degrade multiple components of the extracellular matrix (ECM). MMP-3 can degrade collagen III, IV, V, IX, elastin, laminin and fibronectin, and thus participates in clearance of fibrosis (tissue remodeling). MMPs in general are known to participate in numerous healing and pathologic processes, and changes in plasma levels have been correlated with disease progression and mortality. For example, MMP-3 is often elevated in the circulation of subjects with rheumatologic disease (44), diabetes (82), and cancer (38), but has been found to be lower in the setting of acute myocardial infarct, when activation of fibrosis helps stabilize infarcted cardiac tissue (64, 65). Increased levels of MMP-3 after acute MI are associated with increased adverse cardiac remodeling and death (41). Chronic inhalation of EV led to diminished circulating levels of MMP-3, with a 5.29-fold decrease in C57BL/6 mice, and an 8.42-fold decrease in CD-1 mice (Table 1). Studies have found that knocking out MMP-3 leads to increased tumor growth and metastases, with reduced tumor infiltration of innate immune cells (55). Thus, diminished circulating MMP-3 in EV mice may indicate that organ injury due to chronic EV inhalation is occurring and is leading to activation of fibrosis pathways. But these lower levels of MMP-3 may also be evidence of increased risk of carcinogenesis.

Chitinase 3-like 1 (YKL-40) was decreased 38.9-fold in C57BL/6, and 1.22-fold decreased in CD-1 mice. Chitinase 3-like 1 is also elevated in neutrophilic inflammation and is thought to be secreted more by pro-inflammatory macrophage phenotypes, and less so by anti-inflammatory macrophages (50). One hypothesis of why YKL-40 is diminished in the setting of chronic EV

inhalation is that the nicotine within the EV activated anti-inflammatory pathways (11), leading to a shift to anti-inflammatory monocytes in the circulation.

WISP-1 is associated with pathologic processes including inflammation, tissue repair, and cancer (26). WISP-1 was decreased 2.15-fold in C57BL/6, and 1.49-fold decreased in CD-1 mice. However, the significance of these changes is unclear, as elevated circulating WISP-1 has been associated with renal fibrosis (85) and in cancer studies, WISP-1 levels tend to be elevated as well (53, 80).

One of the limitations of our studies was the use of pooled plasma samples from CD-1 mice for the proteome array studies, as pooling of samples can mask biological variance. We focused on changes only found in both strains, to increase the likelihood of detecting changes associated with the organ fibrosis seen in both strains. Further studies will be needed to assess the biological importance of the differences found, and determine the mechanistic underpinnings.

Relevance of our data to human e-cigarette vapers

These studies were done with commercially purchased e-cigarette batteries, tanks and e-liquids, with puff topography for *in vivo* studies based off of current use patterns to best mimic human use. We included the most common ingredients found in e-liquids: PG, Gly and nicotine. Thus, humans using the same or similar devices (Vape pens) and e-liquids could be at risk for the effects seen in our models. However, because of the wide variety of e-cigarette devices and e-liquids on the market, and the variability across batches, our findings from one brand may not be

relevant to e-cigarette users (vapers) of other types of e-cigarettes, e-cigarettes from other batches or other sources, or even the same devices but at different resistance or voltage (10). E-cigarette researchers across the world are working to develop guidelines to increase consistency across studies, and increase our ability to compare e-cigarette studies to one another (33).

Many investigators work primarily with male mice, as they tend to be more susceptible to organ damage. Therefore, the finding of multi-organ fibrosis in female mice could represent an important pre-clinical signal. Because there are many sex-related disparities in biomedical research, and in murine research in particular, the studies presented here will need to be replicated in male mice to determine whether the findings are relevant across sexes. C57BL/6 mice are the most commonly used strain for basic science research, and many cigarette smoke exposure studies have been completed in this emphysema-susceptible strain (6, 67). Outbred CD-1 mice are more genetically diverse and thus are a hardier strain. Because of their added genetic diversity, significant findings in CD-1 mice may be more relevant to human pathophysiology (Figures 1A, 4 and 5). The fact that we found organ fibrosis in both, genetically disparate, strains of mice, suggests that our results may have a greater likelihood of translatability to humans.

The studies discussed here are limited in that they were done in mice, and there are many known disparities between murine and human inflammatory responses and disease pathology (66). Exposures were done for 1 hour daily, which is a limited pattern of e-cigarette use compared with that of humans, whom more commonly inhale EV for short periods of time throughout the day (20). Nonetheless the fact that changes were observed with only once daily exposure suggests that even larger changes in the same parameters might accompany multiple daily

dosing. Finally, this work was done with e-liquid containing all three of the ingredients found in most e-liquids – PG, Gly and nicotine – and thus we cannot discriminate between them in terms of which may be driving the pathology seen. Further research is needed to evaluate the potential effects of each individual component.

Role of airway epithelium in systemic effects of e-cigarettes

Airway cells, including bronchial epithelial cells, are the first line of defense and protect the host from toxic inhalants. Epithelial permeability is critical for tissue homeostasis (27). The use of e-cigarettes causes modulation of innate immune homeostasis and alters inflammatory cytokine expression. The decreased expression of tight junction protein ZO1 and increased permeability of bronchial epithelial cells can give components of EV access to the systemic circulation, by which they can interact with other tissues to generate fibrosis, as observed clearly here. In addition, the decreased barrier function may allow greater passage of external antigens and inhaled chemicals into the body, increasing inflammation both locally in the lungs and systemically. The further worsening of EV exposed airway epithelial barrier function in the setting of infection suggests that vaping may allow easier entry for pathogens into the lung parenchyma and circulation. This may lead to increased rates of invasive bacterial infections in e-cig users. These studies were limited by the relatively acute *ex vivo* exposure over 3-5 days. Further studies are needed to determine whether tight junction and permeability changes persist in the chronic setting, *in vivo*.

Perspectives and Significance

Our findings of multi-organ dysfunction and fibrosis induced by regular inhalation of EV produced by vape pens illustrate the need to expand clinical, epidemiological, and basic science research studies to include possible effects on organ systems outside of the pulmonary system. Our findings of significant pathophysiologic affects caused by inhalation of non-flavored EV give credence to the belief that there are toxic effects of EV components, beyond those of flavorings alone. The data presented here highlight the need to devote more resources to study these increasingly popular nicotine delivery devices.

Acknowledgements

We would like to thank Lauren Ma, Rita Al-kolla, Albert Tran, and Stefanie Ung for their help and dedication in exposing mice daily. Thanks also to Miriam Scadeng, PhD, who contributed significant *in vivo* MRI imaging time and effort, and Atul Malhotra, MD, for his support and mentorship.

Grants

This work was funded by an American Heart Association Beginning Grant-in-Aid (PI Crotty Alexander 16BGIA27790079), a UAB-UCSD O'Brien Center Daniel O'Connor Scholar Award (PI Crotty Alexander NIH P30-DK079337), a VA BLR&D Career Development Award (PI Crotty Alexander 1IK2BX001313), an ATS Foundation Award (PI Crotty Alexander), a VA Merit (PI Prabhleen Singh BX002175), two R01s (PI Prabhleen Singh DK107852 and PI Crotty Alexander HL137052-01), an R03 (PI Prabhleen Singh DK101841), an R37 (PI Heller Brown R37HL028143), a P01 (Heller Brown P01HL080101), and a F32-DK104615 to Christopher

Drummond. The funding sources had no role in experimental design, collection, analysis or interpretation of the data, writing of the manuscript, or in the decision to submit the paper for publication.

Disclosures

The authors have no conflicts of interest to disclose.

Author Contributions

Conception and design: LCA, EB, PS, SD and CAD. Acquisition, analysis, and interpretation of data: CAD, LCA, JT, SD, MH, AD, AM, JS, PS, JHB, AW, ZY, DM, KV, JL and CJ. Drafting the manuscript for important intellectual content: LCA, EB, JHB and CAD. All authors reviewed, contributed to, and approved the manuscript.

References

1. **Alasmari F, Crotty Alexander LE, Nelson JA, Schiefer IT, Breen E, Drummond CA, and Sari Y**. Effects of chronic inhalation of electronic cigarettes containing nicotine on glial glutamate transporters and alpha-7 nicotinic acetylcholine receptor in female CD-1 mice. *Prog Neuropsychopharmacol Biol Psychiatry* 77: 1-8, 2017.
2. **Ambrose JA, and Barua RS**. The pathophysiology of cigarette smoking and cardiovascular disease: an update. *J Am Coll Cardiol* 43: 1731-1737, 2004.
3. **Apaijai N, Inthachai T, Lekawanvijit S, Chattipakorn SC, and Chattipakorn N**. Effects of dipeptidyl peptidase-4 inhibitor in insulin-resistant rats with myocardial infarction. *J Endocrinol* 229: 245-258, 2016.
4. **Balamayooran G, Batra S, Cai S, Mei J, Worthen GS, Penn AL, and Jeyaseelan S**. Role of CXCL5 in leukocyte recruitment to the lungs during secondhand smoke exposure. *Am J Respir Cell Mol Biol* 47: 104-111, 2012.
5. **Balloy V, Varet H, Dillies MA, Proux C, Jagla B, Coppee JY, Tabary O, Corvol H, Chignard M, and Guillot L**. Normal and Cystic Fibrosis Human Bronchial Epithelial Cells Infected with Pseudomonas aeruginosa Exhibit Distinct Gene Activation Patterns. *PLoS One* 10: e0140979, 2015.

6. **Bartalesi B, Cavarra E, Fineschi S, Lucattelli M, Lunghi B, Martorana PA, and Lungarella G**. Different lung responses to cigarette smoke in two strains of mice sensitive to oxidants. *Eur Respir J* 25: 15-22, 2005.
7. **Behar RZ, Hua M, and Talbot P**. Puffing topography and nicotine intake of electronic cigarette users. *PLoS One* 10: e0117222, 2015.
8. **Bishop JE, and Lindahl G**. Regulation of cardiovascular collagen synthesis by mechanical load. *Cardiovasc Res* 42: 27-44, 1999.
9. **Bolinder G, Alfredsson L, Englund A, and de Faire U**. Smokeless tobacco use and increased cardiovascular mortality among Swedish construction workers. *Am J Public Health* 84: 399-404, 1994.
10. **Brown CJ, and Cheng JM**. Electronic cigarettes: product characterisation and design considerations. *Tob Control* 23 Suppl 2: ii4-10, 2014.
11. **Cafe-Mendes CC, Garay-Malpartida HM, Malta MB, de Sa Lima L, Scavone C, Ferreira ZS, Markus RP, and Marcourakis T**. Chronic nicotine treatment decreases LPS signaling through NF-kappaB and TLR-4 modulation in the hippocampus. *Neurosci Lett* 636: 218-224, 2017.
12. **Caponnetto P, Campagna D, Papale G, Russo C, and Polosa R**. The emerging phenomenon of electronic cigarettes. *Expert Rev Respir Med* 6: 63-74, 2012.
13. **Carson JL, Brighton LE, Collier AM, and Bromberg PA**. Correlative ultrastructural investigations of airway epithelium following experimental exposure to defined air pollutants and lifestyle exposure to tobacco smoke. *Inhal Toxicol* 25: 134-140, 2013.
14. **Cavarra E, Bartalesi B, Lucattelli M, Fineschi S, Lunghi B, Gambelli F, Ortiz LA, Martorana PA, and Lungarella G**. Effects of cigarette smoke in mice with different levels of alpha(1)-proteinase inhibitor and sensitivity to oxidants. *Am J Respir Crit Care Med* 164: 886-890, 2001.
15. **Chen JX, and Stinnett A**. Ang-1 gene therapy inhibits hypoxia-inducible factor-1alpha (HIF-1alpha)-prolyl-4-hydroxylase-2, stabilizes HIF-1alpha expression, and normalizes immature vasculature in db/db mice. *Diabetes* 57: 3335-3343, 2008.
16. **Clark CA, Thomas LK, and Azghani AO**. Inhibition of protein kinase C attenuates Pseudomonas aeruginosa elastase-induced epithelial barrier disruption. *Am J Respir Cell Mol Biol* 45: 1263-1271, 2011.
17. **Crotty Alexander L, Fuster M, Montgrain P, and Malhotra A**. The Need for More E-Cigarette Data: A Call to Action. *Am J Respir Crit Care Med* 192: 275-276, 2015.
18. **Crotty Alexander LE, Shin S, and Hwang JH**. Inflammatory Diseases of the Lung Induced by Conventional Cigarette Smoke: A Review. *Chest* 148: 1307-1322, 2015.
19. **Crotty Alexander LE, Vyas A, Schraufnagel DE, and Malhotra A**. Electronic cigarettes: the new face of nicotine delivery and addiction. *J Thorac Dis* 7: E248-251, 2015.
20. **Dawkins L, Turner J, Roberts A, and Soar K**. 'Vaping' profiles and preferences: an online survey of electronic cigarette users. *Addiction* 108: 1115-1125, 2013.
21. **Drummond CA, Crotty Alexander LE, Haller ST, Fan X, Xie JX, Kennedy DJ, Liu J, Yan Y, Hernandez DA, Mathew DP, Cooper CJ, Shapiro JI, and Tian J**. Cigarette Smoking Causes Epigenetic Changes Associated With Cardiorenal Fibrosis. *Physiol Genomics* physiolgenomics 00070 02016, 2016.
22. **Drummond CA, Hill MC, Shi H, Fan X, Xie JX, Haller ST, Kennedy DJ, Liu J, Garrett MR, Xie Z, Cooper CJ, Shapiro JI, and Tian J**. Na/K-ATPase signaling regulates collagen synthesis through microRNA-29b-3p in cardiac fibroblasts. *Physiol Genomics* 48: 220-229, 2016.
23. **Drummond CA, Sayed M, Evans KL, Shi H, Wang X, Haller ST, Liu J, Cooper CJ, Xie Z, Shapiro JI, and Tian J**. Reduction of Na/K-ATPase affects cardiac remodeling and increases c-kit cell abundance in partial nephrectomized mice. *American journal of physiology Heart and circulatory physiology* 306: H1631-1643, 2014.
24. **Eddy AA**. Overview of the cellular and molecular basis of kidney fibrosis. *Kidney Int Suppl (2011)* 4: 2-8, 2014.

25. **Etter JF**. A longitudinal study of cotinine in long-term daily users of e-cigarettes. *Drug Alcohol Depend* 160: 218-221, 2016.
26. **Feng M, and Jia S**. Dual effect of WISP-1 in diverse pathological processes. *Chin J Cancer Res* 28: 553-560, 2016.
27. **Ganesan S, Comstock AT, and Sajjan US**. Barrier function of airway tract epithelium. *Tissue Barriers* 1: e24997, 2013.
28. **Golli NE, Jrad-Lamine A, Neffati H, Dkhili H, Rahali D, Dallagi Y, El May MV, and El Fazaa S**. Impact of e-cigarette refill liquid exposure on rat kidney. *Regul Toxicol Pharmacol* 77: 109-116, 2016.
29. **Guerassimov A, Hoshino Y, Takubo Y, Turcotte A, Yamamoto M, Ghezzo H, Triantafillopoulos A, Whittaker K, Hoidal JR, and Cosio MG**. The development of emphysema in cigarette smoke-exposed mice is strain dependent. *Am J Respir Crit Care Med* 170: 974-980, 2004.
30. **Gupta RK, Gupta R, Maheshwari VD, and Mawliya M**. Impact of smoking on microalbuminuria and urinary albumin creatinine ratio in non-diabetic normotensive smokers. *Indian J Nephrol* 24: 92-96, 2014.
31. **Haller ST, Kennedy DJ, Shidyak A, Budny GV, Malhotra D, Fedorova OV, Shapiro JI, and Bagrov AY**. Monoclonal antibody against marinobufagenin reverses cardiac fibrosis in rats with chronic renal failure. *American journal of hypertension* 25: 690-696, 2012.
32. **Hwang JH, Lyes M, Sladewski K, Enany S, McEachern E, Mathew DP, Das S, Moshensky A, Bapat S, Pride DT, Ongkeko WM, and Crotty Alexander LE**. Electronic cigarette inhalation alters innate immunity and airway cytokines while increasing the virulence of colonizing bacteria. *J Mol Med (Berl)* 2016.
33. **Iskandar AR, Gonzalez-Suarez I, Majeed S, Marescotti D, Sewer A, Xiang Y, Leroy P, Guedj E, Mathis C, Schaller JP, Vanscheeuwijck P, Frentzel S, Martin F, Ivanov NV, Peitsch MC, and Hoeng J**. A framework for in vitro systems toxicology assessment of e-liquids. *Toxicol Mech Methods* 26: 389-413, 2016.
34. **Jensen RP, Luo W, Pankow JF, Strongin RM, and Peyton DH**. Hidden formaldehyde in e-cigarette aerosols. *N Engl J Med* 372: 392-394, 2015.
35. **Jeyaseelan S, Manzer R, Young SK, Yamamoto M, Akira S, Mason RJ, and Worthen GS**. Induction of CXCL5 during inflammation in the rodent lung involves activation of alveolar epithelium. *Am J Respir Cell Mol Biol* 32: 531-539, 2005.
36. **Jones JA, Stroud RE, O'Quinn EC, Black LE, Barth JL, Elefteriades JA, Bavaria JE, Gorman JH, 3rd, Gorman RC, Spinale FG, and Ikonomidis JS**. Selective microRNA suppression in human thoracic aneurysms: relationship of miR-29a to aortic size and proteolytic induction. *Circulation Cardiovascular genetics* 4: 605-613, 2011.
37. **Jung GS, Jeon JH, Choe MS, Kim SW, Lee IK, Kim MK, and Park KG**. Renoprotective Effect of Gemigliptin, a Dipeptidyl Peptidase-4 Inhibitor, in Streptozotocin-Induced Type 1 Diabetic Mice. *Diabetes Metab J* 40: 211-221, 2016.
38. **Jung K, Nowak L, Lein M, Priem F, Schnorr D, and Loening SA**. Matrix metalloproteinases 1 and 3, tissue inhibitor of metalloproteinase-1 and the complex of metalloproteinase-1/tissue inhibitor in plasma of patients with prostate cancer. *Int J Cancer* 74: 220-223, 1997.
39. **Kalkhoran S, and Glantz SA**. E-cigarettes and smoking cessation in real-world and clinical settings: a systematic review and meta-analysis. *Lancet Respir Med* 4: 116-128, 2016.
40. **Kanasaki K, Shi S, Kanasaki M, He J, Nagai T, Nakamura Y, Ishigaki Y, Kitada M, Srivastava SP, and Koya D**. Linagliptin-mediated DPP-4 inhibition ameliorates kidney fibrosis in streptozotocin-induced diabetic mice by inhibiting endothelial-to-mesenchymal transition in a therapeutic regimen. *Diabetes* 63: 2120-2131, 2014.

41. **Kelly D, Khan S, Cockerill G, Ng LL, Thompson M, Samani NJ, and Squire IB**. Circulating stromelysin-1 (MMP-3): a novel predictor of LV dysfunction, remodelling and all-cause mortality after acute myocardial infarction. *Eur J Heart Fail* 10: 133-139, 2008.
42. **Kennedy DJ, Elkareh J, Shidyak A, Shapiro AP, Smaili S, Mutgi K, Gupta S, Tian J, Morgan E, Khouri S, Cooper CJ, Periyasamy SM, Xie Z, Malhotra D, Fedorova OV, Bagrov AY, and Shapiro JI**. Partial nephrectomy as a model for uremic cardiomyopathy in the mouse. *American journal of physiology Renal physiology* 294: F450-454, 2008.
43. **Kennedy DJ, Vetteth S, Periyasamy SM, Kanj M, Fedorova L, Khouri S, Kahaleh MB, Xie Z, Malhotra D, Kolodkin NI, Lakatta EG, Fedorova OV, Bagrov AY, and Shapiro JI**. Central role for the cardiotonic steroid marinobufagenin in the pathogenesis of experimental uremic cardiomyopathy. *Hypertension* 47: 488-495, 2006.
44. **Keyszer G, Lambiri I, Nagel R, Keysser C, Keysser M, Gromnica-Ihle E, Franz J, Burmester GR, and Jung K**. Circulating levels of matrix metalloproteinases MMP-3 and MMP-1, tissue inhibitor of metalloproteinases 1 (TIMP-1), and MMP-1/TIMP-1 complex in rheumatic disease. Correlation with clinical activity of rheumatoid arthritis versus other surrogate markers. *J Rheumatol* 26: 251-258, 1999.
45. **Kierszniewska-Stepien D, Pietras T, Ciebiada M, Gorski P, and Stepien H**. Concentration of angiopoietins 1 and 2 and their receptor Tie-2 in peripheral blood in patients with chronic obstructive pulmonary disease. *Postepy Dermatol Alergol* 32: 443-448, 2015.
46. **Kim W, Moon SO, Lee SY, Jang KY, Cho CH, Koh GY, Choi KS, Yoon KH, Sung MJ, Kim DH, Lee S, Kang KP, and Park SK**. COMP-angiopoietin-1 ameliorates renal fibrosis in a unilateral ureteral obstruction model. *J Am Soc Nephrol* 17: 2474-2483, 2006.
47. **Knight DA, Lydell CP, Zhou D, Weir TD, Robert Schellenberg R, and Bai TR**. Leukemia inhibitory factor (LIF) and LIF receptor in human lung. Distribution and regulation of LIF release. *Am J Respir Cell Mol Biol* 20: 834-841, 1999.
48. **Kriegel AJ, Liu Y, Cohen B, Usa K, Liu Y, and Liang M**. MiR-382 targeting of kallikrein 5 contributes to renal inner medullary interstitial fibrosis. *Physiol Genomics* 44: 259-267, 2012.
49. **Kruschinski C, Skripuletz T, Bedoui S, Tschernig T, Pabst R, Nassenstein C, Braun A, and von Horsten S**. CD26 (dipeptidyl-peptidase IV)-dependent recruitment of T cells in a rat asthma model. *Clin Exp Immunol* 139: 17-24, 2005.
50. **Kunz LI, van't Wout EF, van Schadewijk A, Postma DS, Kerstjens HA, Sterk PJ, and Hiemstra PS**. Regulation of YKL-40 expression by corticosteroids: effect on pro-inflammatory macrophages in vitro and its modulation in COPD in vivo. *Respir Res* 16: 154, 2015.
51. **Larcombe AN, Janka MA, Mullins BJ, Berry LJ, Bredin A, and Franklin PJ**. The effects of electronic cigarette aerosol exposure on inflammation and lung function in mice. *Am J Physiol Lung Cell Mol Physiol* ajplung 00203 02016, 2017.
52. **Lever AR, Park H, Mulhern TJ, Jackson GR, Comolli JC, Borenstein JT, Hayden PJ, and Prantil-Baun R**. Comprehensive evaluation of poly(I:C) induced inflammatory response in an airway epithelial model. *Physiol Rep* 3: 2015.
53. **Li FJ, Wang XJ, and Zhou XL**. WISP-1 overexpression upregulates cell proliferation in human salivary gland carcinomas via regulating MMP-2 expression. *Onco Targets Ther* 9: 6539-6548, 2016.
54. **McCauley L, Markin C, and Hosmer D**. An unexpected consequence of electronic cigarette use. *Chest* 141: 1110-1113, 2012.
55. **McCawley LJ, Crawford HC, King LE, Jr., Mudgett J, and Matrisian LM**. A protective role for matrix metalloproteinase-3 in squamous cell carcinoma. *Cancer Res* 64: 6965-6972, 2004.
56. **Mercado C, and Jaimes EA**. Cigarette smoking as a risk factor for atherosclerosis and renal disease: novel pathogenic insights. *Curr Hypertens Rep* 9: 66-72, 2007.
57. **Mukherjee D, and Sen S**. Alteration of collagen phenotypes in ischemic cardiomyopathy. *J Clin Invest* 88: 1141-1146, 1991.

58. **Negri E, Franzosi MG, La Vecchia C, Santoro L, Nobili A, and Tognoni G**. Tar yield of cigarettes and risk of acute myocardial infarction. GISSI-EFRIM Investigators. *BMJ* 306: 1567-1570, 1993.
59. **Olivera DS, Boggs SE, Beenhouwer C, Aden J, and Knall C**. Cellular mechanisms of mainstream cigarette smoke-induced lung epithelial tight junction permeability changes in vitro. *Inhal Toxicol* 19: 13-22, 2007.
60. **Orosz Z, Csiszar A, Labinskyy N, Smith K, Kaminski PM, Ferdinandy P, Wolin MS, Rivera A, and Ungvari Z**. Cigarette smoke-induced proinflammatory alterations in the endothelial phenotype: role of NAD(P)H oxidase activation. *Am J Physiol Heart Circ Physiol* 292: H130-139, 2007.
61. **Qiu Y, Zhu J, Bandi V, Atmar RL, Hattotuwa K, Guntupalli KK, and Jeffery PK**. Biopsy neutrophilia, neutrophil chemokine and receptor gene expression in severe exacerbations of chronic obstructive pulmonary disease. *Am J Respir Crit Care Med* 168: 968-975, 2003.
62. **Ren SG, Seliktar J, Li X, Braunstein GD, and Melmed S**. Measurement of leukemia inhibitory factor in biological fluids by radioimmunoassay. *J Clin Endocrinol Metab* 83: 1275-1283, 1998.
63. **Righetti M, and Sessa A**. Cigarette smoking and kidney involvement. *J Nephrol* 14: 3-6, 2001.
64. **Samnegard A, Silveira A, Lundman P, Boquist S, Odeberg J, Hulthe J, McPheat W, Tornvall P, Bergstrand L, Ericsson CG, Hamsten A, and Eriksson P**. Serum matrix metalloproteinase-3 concentration is influenced by MMP-3 -1612 5A/6A promoter genotype and associated with myocardial infarction. *J Intern Med* 258: 411-419, 2005.
65. **Samnegard A, Silveira A, Tornvall P, Hamsten A, Ericsson CG, and Eriksson P**. Lower serum concentration of matrix metalloproteinase-3 in the acute stage of myocardial infarction. *J Intern Med* 259: 530-536, 2006.
66. **Seok J, Warren HS, Cuenca AG, Mindrinos MN, Baker HV, Xu W, Richards DR, McDonald-Smith GP, Gao H, Hennessy L, Finnerty CC, Lopez CM, Honari S, Moore EE, Minei JP, Cuschieri J, Bankey PE, Johnson JL, Sperry J, Nathens AB, Billiar TR, West MA, Jeschke MG, Klein MB, Gamelli RL, Gibran NS, Brownstein BH, Miller-Graziano C, Calvano SE, Mason PH, Cobb JP, Rahme LG, Lowry SF, Maier RV, Moldawer LL, Herndon DN, Davis RW, Xiao W, Tompkins RG, Inflammation, and Host Response to Injury LSCRP**. Genomic responses in mouse models poorly mimic human inflammatory diseases. *Proc Natl Acad Sci U S A* 110: 3507-3512, 2013.
67. **Shapiro SD, Goldstein NM, Houghton AM, Kobayashi DK, Kelley D, and Belaaouaj A**. Neutrophil elastase contributes to cigarette smoke-induced emphysema in mice. *Am J Pathol* 163: 2329-2335, 2003.
68. **Shaykhiev R, Otaki F, Bonsu P, Dang DT, Teater M, Strulovici-Barel Y, Salit J, Harvey BG, and Crystal RG**. Cigarette smoking reprograms apical junctional complex molecular architecture in the human airway epithelium in vivo. *Cell Mol Life Sci* 68: 877-892, 2011.
69. **Shi S, Koya D, and Kanasaki K**. Dipeptidyl peptidase-4 and kidney fibrosis in diabetes. *Fibrogenesis Tissue Repair* 9: 1, 2016.
70. **Singh S, Manson SR, Lee H, Kim Y, Liu T, Guo Q, Geminiani JJ, Austin PF, and Chen YM**. Tubular Overexpression of Angiopoietin-1 Attenuates Renal Fibrosis. *PLoS One* 11: e0158908, 2016.
71. **Skripuletz T, Schmiedl A, Schade J, Bedoui S, Glaab T, Pabst R, von Horsten S, and Stephan M**. Dose-dependent recruitment of CD25+ and CD26+ T cells in a novel F344 rat model of asthma. *Am J Physiol Lung Cell Mol Physiol* 292: L1564-1571, 2007.
72. **Sleiman M, Logue JM, Montesinos VN, Russell ML, Litter MI, Gundel LA, and Destaillats H**. Emissions from Electronic Cigarettes: Key Parameters Affecting the Release of Harmful Chemicals. *Environ Sci Technol* 50: 9644-9651, 2016.
73. **Steinbrecher A, Reinhold D, Quigley L, Gado A, Tresser N, Izikson L, Born I, Faust J, Neubert K, Martin R, Ansorge S, and Brocke S**. Targeting dipeptidyl peptidase IV (CD26) suppresses autoimmune encephalomyelitis and up-regulates TGF-beta 1 secretion in vivo. *J Immunol* 166: 2041-2048, 2001.
74. **Sukhija R, Bursac Z, Kakar P, Fink L, Fort C, Satwani S, Aronow WS, Bansal D, and Mehta JL**. Effect of statins on the development of renal dysfunction. *Am J Cardiol* 101: 975-979, 2008.

75. **Sussan TE, Gajghate S, Thimmulappa RK, Ma J, Kim JH, Sudini K, Consolini N, Cormier SA, Lomnicki S, Hasan F, Pekosz A, and Biswal S**. Exposure to electronic cigarettes impairs pulmonary anti-bacterial and anti-viral defenses in a mouse model. *PLoS One* 10: e0116861, 2015.
76. **Thota D, and Latham E**. Case report of electronic cigarettes possibly associated with eosinophilic pneumonitis in a previously healthy active-duty sailor. *J Emerg Med* 47: 15-17, 2014.
77. **Uchiyama S, Senoo Y, Hayashida H, Inaba Y, Nakagome H, and Kunugita N**. Determination of Chemical Compounds Generated from Second-generation E-cigarettes Using a Sorbent Cartridge Followed by a Two-step Elution Method. *Anal Sci* 32: 549-555, 2016.
78. **Wang J, Chen Q, Corne J, Zhu Z, Lee CG, Bhandari V, Homer RJ, and Elias JA**. Pulmonary expression of leukemia inhibitory factor induces B cell hyperplasia and confers protection in hyperoxia. *J Biol Chem* 278: 31226-31232, 2003.
79. **Wu Q, Jiang D, Minor M, and Chu HW**. Electronic cigarette liquid increases inflammation and virus infection in primary human airway epithelial cells. *PLoS One* 9: e108342, 2014.
80. **Yang JY, Yang MW, Huo YM, Liu W, Liu DJ, Li J, Zhang JF, Hua R, and Sun YW**. High expression of WISP-1 correlates with poor prognosis in pancreatic ductal adenocarcinoma. *Am J Transl Res* 7: 1621-1628, 2015.
81. **Yu V, Rahimy M, Korrapati A, Xuan Y, Zou AE, Krishnan AR, Tsui T, Aguilera JA, Advani S, Crotty Alexander LE, Brumund KT, Wang-Rodriguez J, and Ongkeko WM**. Electronic cigarettes induce DNA strand breaks and cell death independently of nicotine in cell lines. *Oral Oncol* 52: 58-65, 2016.
82. **Zakovicova E, Charvat J, Kukacka J, Chlumsky J, Svab P, and Kvapil M**. Circulating serum matrix metalloproteinase-3 and metalloproteinase-9 are not associated with echocardiographic parameters of diastolic function in asymptomatic type 2 diabetic patients. *J Int Med Res* 38: 2093-2099, 2010.
83. **Zeng H, Li L, and Chen JX**. Overexpression of angiopoietin-1 increases CD133+/c-kit+ cells and reduces myocardial apoptosis in db/db mouse infarcted hearts. *PLoS One* 7: e35905, 2012.
84. **Zhang X, Urbieta-Caceres VH, Eirin A, Bell CC, Crane JA, Tang H, Jordan KL, Oh YK, Zhu XY, Korsmo MJ, Bachar AR, Cohen P, Lerman A, and Lerman LO**. Humanin prevents intra-renal microvascular remodeling and inflammation in hypercholesterolemic ApoE deficient mice. *Life Sci* 91: 199-206, 2012.
85. **Zhong X, Tu YJ, Li Y, Zhang P, Wang W, Chen SS, Li L, Chung AC, Lan HY, Chen HY, Li GS, and Wang L**. Serum levels of WNT1-inducible signaling pathway protein-1 (WISP-1): a noninvasive biomarker of renal fibrosis in subjects with chronic kidney disease. *Am J Transl Res* 9: 2920-2932, 2017.
86. **Zhuge F, Ni Y, Nagashimada M, Nagata N, Xu L, Mukaida N, Kaneko S, and Ota T**. DPP-4 Inhibition by Linagliptin Attenuates Obesity-Related Inflammation and Insulin Resistance by Regulating M1/M2 Macrophage Polarization. *Diabetes* 65: 2966-2979, 2016.

Figure Legends

Figure 1. Diagram of an electronic (e)-cigarette (A). For our *in vitro* model of firsthand EV exposure **(B)**, the e-cigarette hooked up to rubber tubing and a 3-way stopcock, such that negative pressure is applied to the mouthpiece via pulling back the plunger on a 60mL syringe, generating fresh e-cigarette vapor (EV). The syringe is filled with 50mLs of EV each time, and the EV is subsequently exhaled through the side-port of the 3-way stopcock onto primary human airway epithelial cells.

Figure 2. C57BL/6 (A) and CD-1 (B) mice exposed daily to EV for 3 and 6 months, respectively, had modulated levels of inflammatory proteins in the serum, consistent with an altered systemic inflammatory state. Sera were evaluated by 111-cytokine antibody array (Proteome Profiler Mouse XL Array; R&D), and graphed as a ratio of EV/Air for proteins that increased with EV exposure, and Air/EV for proteins that decreased with EV exposure. **A.** Changes in C57BL/6 serum protein levels caused by EV exposure are shown, with a 20% threshold in either direction, including large rises in Angiopoietin-1 and EGF in EV mice, and much decreased Chitinase 3-like 1 and MMP-3 in EV mice (n = 3 per group). **B.** Serum protein changes in CD-1 mice, including large increases in LIF (murine equivalent of IL-8) and EGF, and large decreases in MMP-3 and WISP-1 (n = 6 per group, pooled). *Protein changes occurred in both CD1 and C57BL/6 mice.

Table 1. Circulating inflammatory proteins that changed in both C57BL/6 and CD-1 mice chronically exposed to EV. Proteins which were elevated in the plasma of EV mice are in blue, and proteins which decreased in the plasma of EV mice are in orange.

Figure 3. Mice that inhaled EV for an hour daily had inflammatory changes only at the protein level. A. Lung parenchyma was stained with H&E and Masson's Trichrome stains. One lung slice per mouse, including large, medium and small airways, was evaluated by a blinded pathologist, and no pulmonary inflammation, emphysema or fibrosis was found in EV mice relative to Air controls (n = 6 per group). **B.** The airways of mice, as measured through BAL, had alterations in the inflammatory cytokine profile. BAL was pooled within EV and Air control groups (n = 6 within groups) and was evaluated by 111-cytokine antibody array (Proteome Profiler Mouse XL Array; R&D), and graphed as a ratio of EV/Air. BAL from EV mice had decreased levels of LIX (murine version of IL-8; 519-fold lower or approximately 0.2% of Air levels) and VCAM-1 (99-fold lower or 1% of Air levels). EV BAL had increased levels of DPPIV (1.7-fold or 58% higher than Air levels).

Figure 4. Primary normal human bronchial epithelial cells (NHBEs) became leaky and pro-inflammatory with daily short 15 minute EV exposures for 2-5 days. A. EV treated NHBE cells tested for permeability with FITC-dextran had greater passage of small molecules, compared with controls exposed to Air only, on both day 2 and day 5 ($p < 0.01$; Mean +/- SEM; wells were run in triplicate). **B.** EV exposed NHBEs secreted more IL-8 than Air controls in response to bacterial infection (37 vs 227 pg/mL, respectively; $p < 0.05$; wells were run in triplicate). **C.** Protein quantification of Western blots of the tight junction protein zona occludins (ZO1) found 3.3-fold lower quantities in NHBEs after EV exposure, as compared with Air controls ($p = 0.024$; $n = 3$). Levels of loading control tubulin were similar across samples ($p = 0.99$).

Figure 5. Chronic EV inhalation diminished cardiorenal function and induced renal fibrosis in C57BL/6 mice exposed to EV for 3 months. A. EV induced a 20% reduction in glomerular filtration rate (GFR) as compared with experimental controls ($p = 0.017$). **B.** Representative Masson's trichrome 20x, Picrosirius Red 20x bright-field and 10x polarized light photomicrographs of renal tissue fibrosis. **C.** Fibrosis was quantified in kidneys from EV and Air mice, by blinded grading of kidney sections. EV kidneys had 87% (1.86-fold increase) more collagen versus experimental controls. When only the 10 sections with the highest levels of collagen staining were compared, EV kidneys still had 1.88-fold higher levels of fibrosis, compared with controls. **D**. Picrosirius red staining also demonstrated higher collagen content in EV exposed mice, relative to Air controls (1.62-fold increase, $p = 0.034$). Mean +/- SEM are shown, $n = 5$-6 per group, $p < 0.05$.

Figure 6. Induction of kidney fibrosis also occurred in CD-1 mice exposed to EV for 6 months. A. Kidney parenchyma stained with Masson's Trichrome and Picrosirius Red stains. **B.** In CD-1 mice, daily EV inhalation for 6 months led to a 3.2-fold increase in renal fibrosis, assessed by Masson's Trichrome stain, relative to air controls (Mean +/- SEM are shown; $p = 0.022$). **C.** Picrosirius red staining also demonstrated 2.14-fold higher collagen content in EV exposed mice, relative to Air controls (Mean +/- SEM are shown; $p < 0.01$). **D-K.** To assess for the origin of fibrosis, genes associated with fibrosis and extracellular matrix pathways were evaluated after only 4-weeks of EV or Air exposure. Lower expression of the anti-fibrotic miRNA miR-29b-3p **(D)** and higher expression of collagen-1 within CD-1 renal parenchyma **(E)**, suggest that fibrosis begins early in the course of daily EV inhalation. The expression of additional pro-fibrotic factors, Col3a1 **(F)**, Col4a1 **(G),** Itgb1 **(I)**, and Fbn1 **(J)**, were all

significantly increased in renal tissues from e-cigarette exposed animals ($p < 0.05$). Extracellular matrix remodeling factor Mmp2 trended up, but not significantly **(H)**. However, the fibrosis component Eln was not significantly different **(K)**. *$p < 0.05$, n = 5-6 for all groups

Figure 7. Chronic inhalation of EV induced cardiac fibrosis and altered cardiovascular function. A. Masson's Trichrome stain of fixed cardiac ventricular tissue from CD-1 mice exposed to EV daily for 6 months. **B.** Quantitative analysis of EV relative to control determined that EV hearts had 2.75-fold greater level of collagen staining in ventricular tissue compared with controls (***$p < 0.001$). **C-D.** When tissues were harvested after only 4 weeks of EV exposure, cardiac tissues were found to have higher expression of collagen-3 mRNA (**C**)**,** but normal expression levels of collagen-1 mRNA (**D**)(*$p < 0.05$). For figures A-D, n = 6 per group. **E.** In C57BL/6 mice, EV daily for 3 months led to decreased heart rates (HR), as compared with air controls ($p < 0.01$). **F.** HR were more variable in EV exposed mice, as indicated by greater standard deviation within beat-to-beat measurements of each mouse. **G.** Systolic blood pressure was increased in e-cigarette exposed mice ($p = 0.016$). **H.** Diastolic blood pressure trended up in EV mice ($p = 0.050$). For figures E-H, n = 19 for EV and n = 20 for Air controls.

Figure 8. **Chronic inhalation of EV led to hepatic fibrosis in CD-1 mice exposed to EV for 6 months. A.** Representative Masson's Trichrome photomicrographs of fixed hepatic tissue. **B.** Quantitative analysis of EV relative to control determined that EV livers exposed to EV daily for 6 months had 1.9-fold higher collagen deposition, relative to Air controls. Mean +/- SEM are shown, n=6 per group. ****$p < 0.0001$

Figure 1

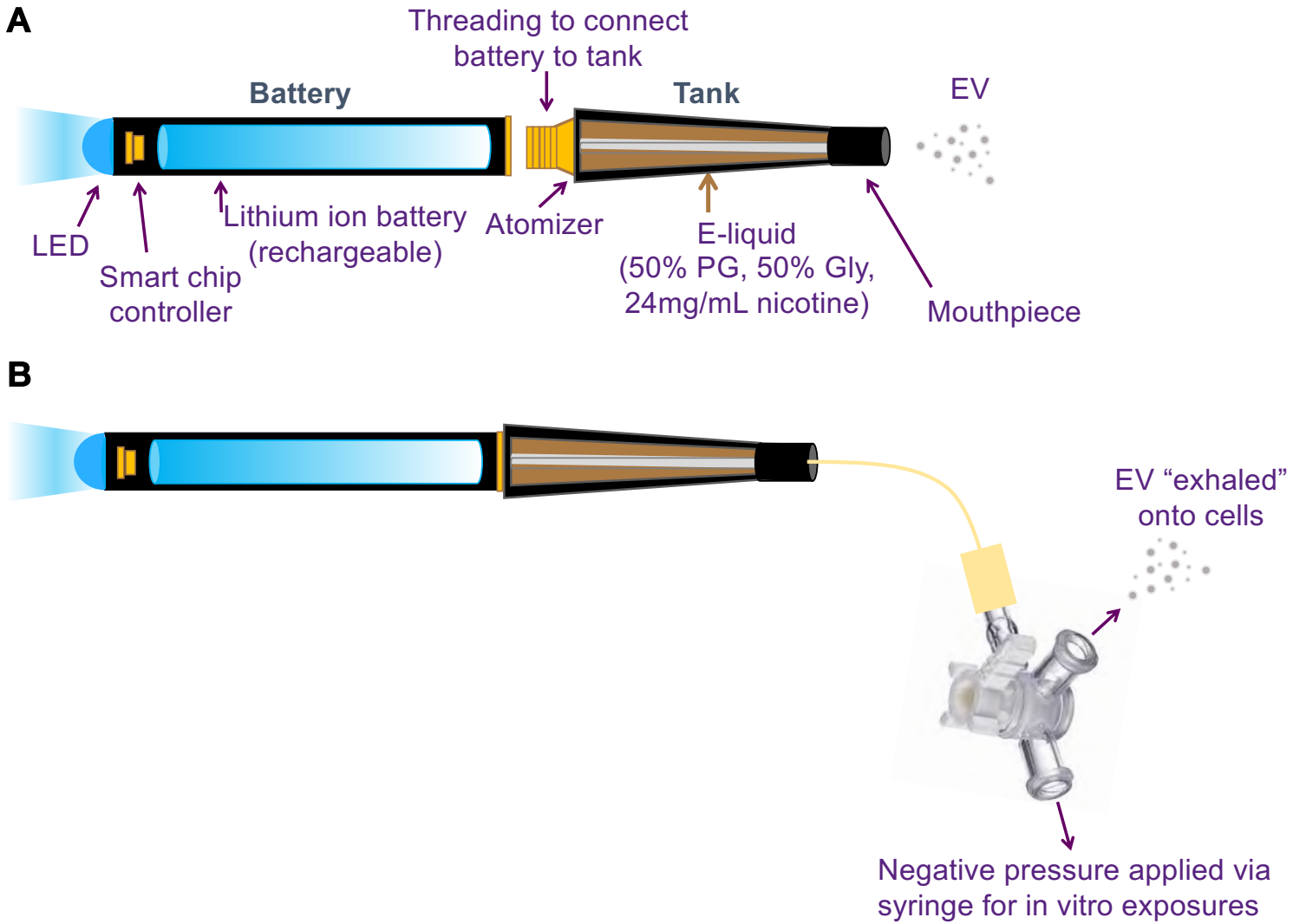

Figure 2

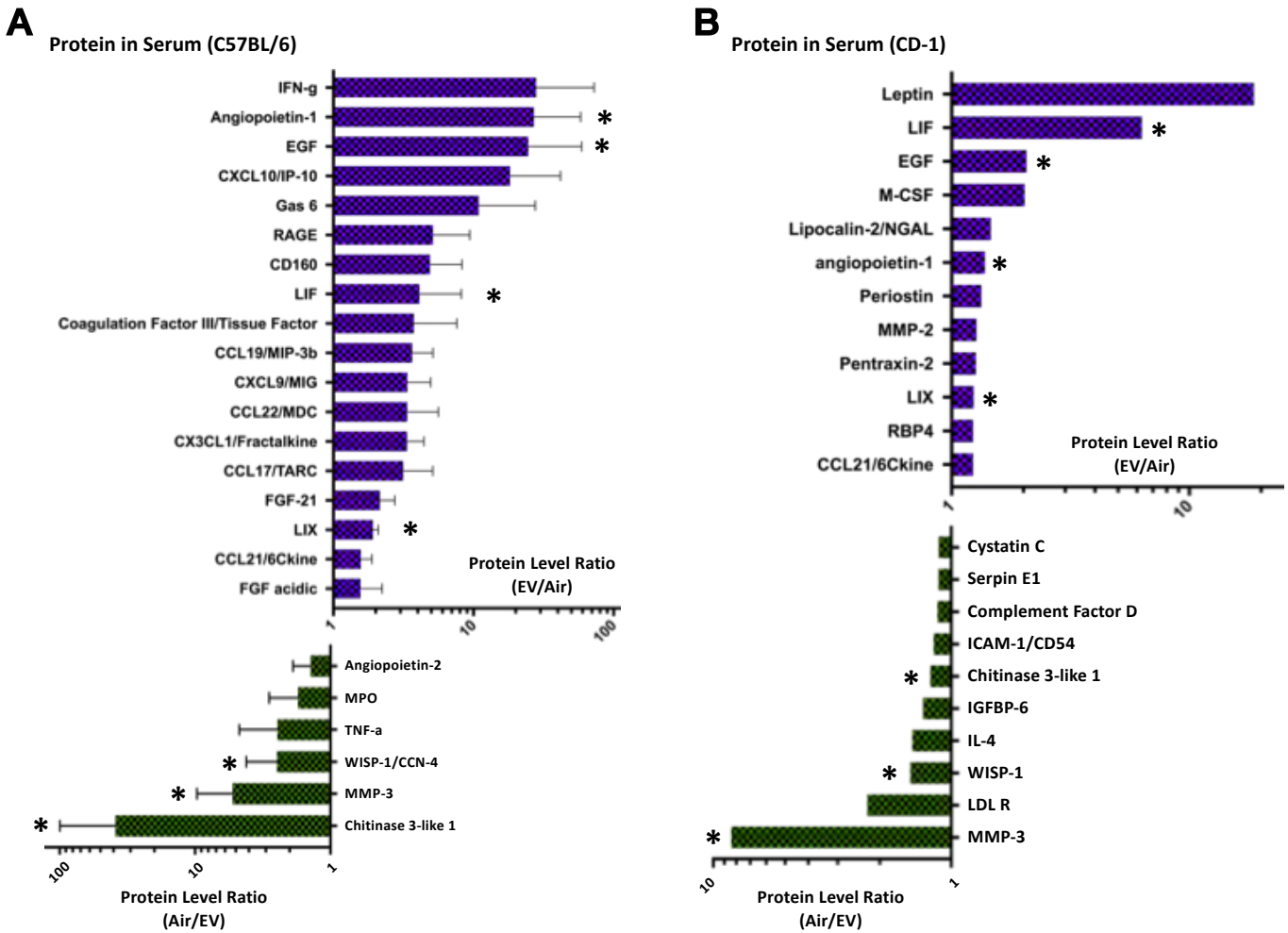

Table 1

Table 1. Circulating inflammatory proteins that changed in both C57BL/6 and CD-1 mice chronically exposed to EV. Proteins which were elevated in the plasma of EV mice are in blue, and proteins which decreased in the plasma of EV mice are in orange.

Protein	Fold change in C57BL/6	Fold change in CD-1
LIF	30.6	6.29
EGF	24.6	2.06
Angiopoietin-1	27	1.38
LIX	1.92	1.24
MMP-3	-5.29	-8.42
Chitinase 3-like 1	-38.9	-1.22
WISP-1	-2.15	-1.49

Figure 3 (A)

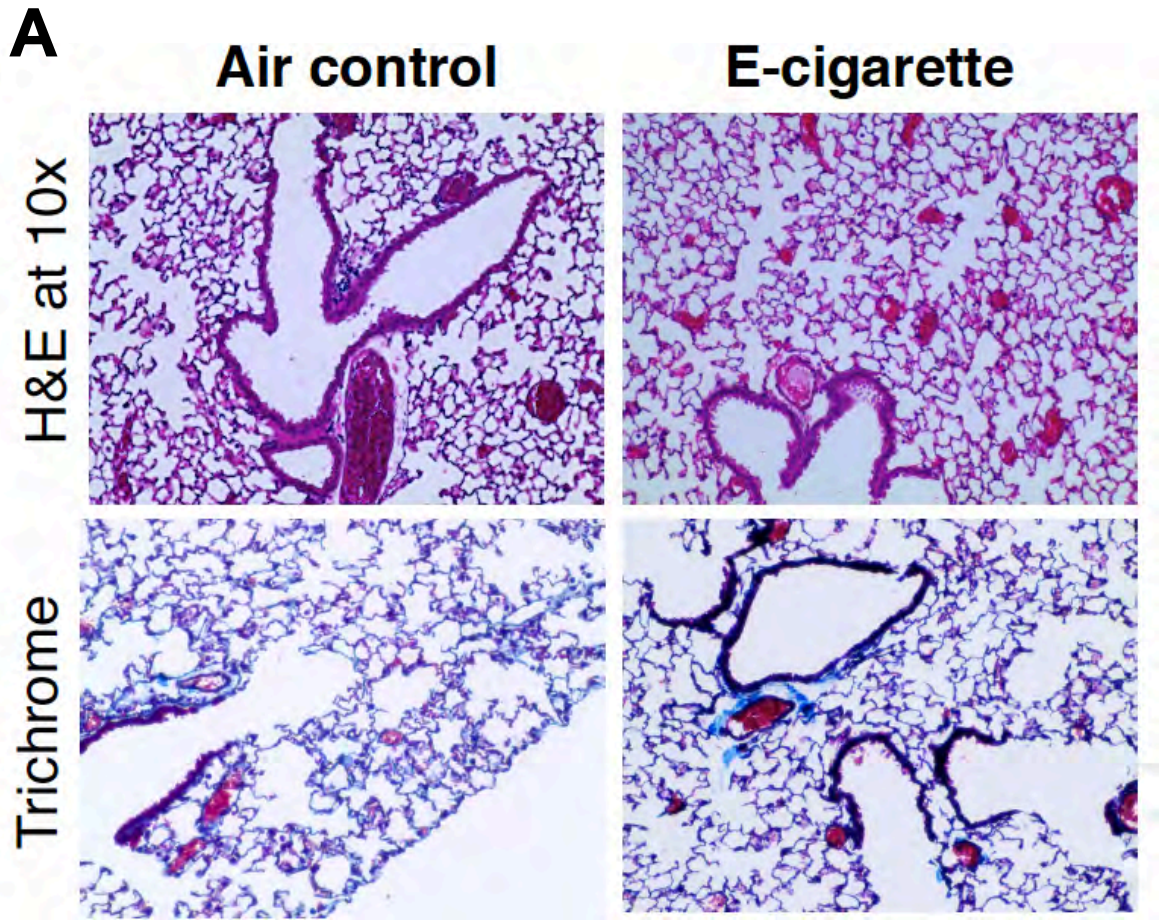

Figure 3 (B)

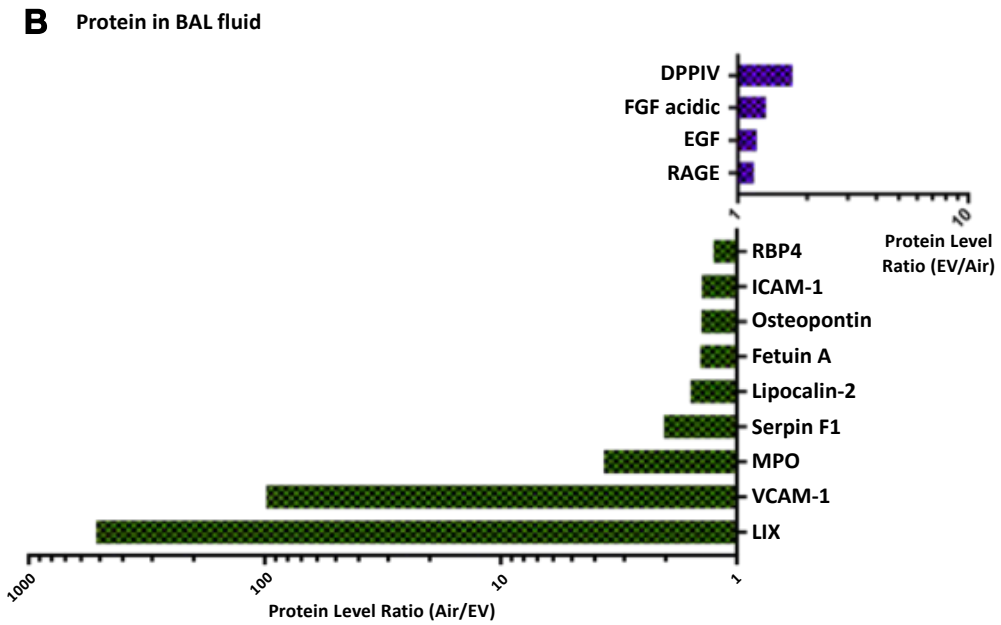

Figure 4

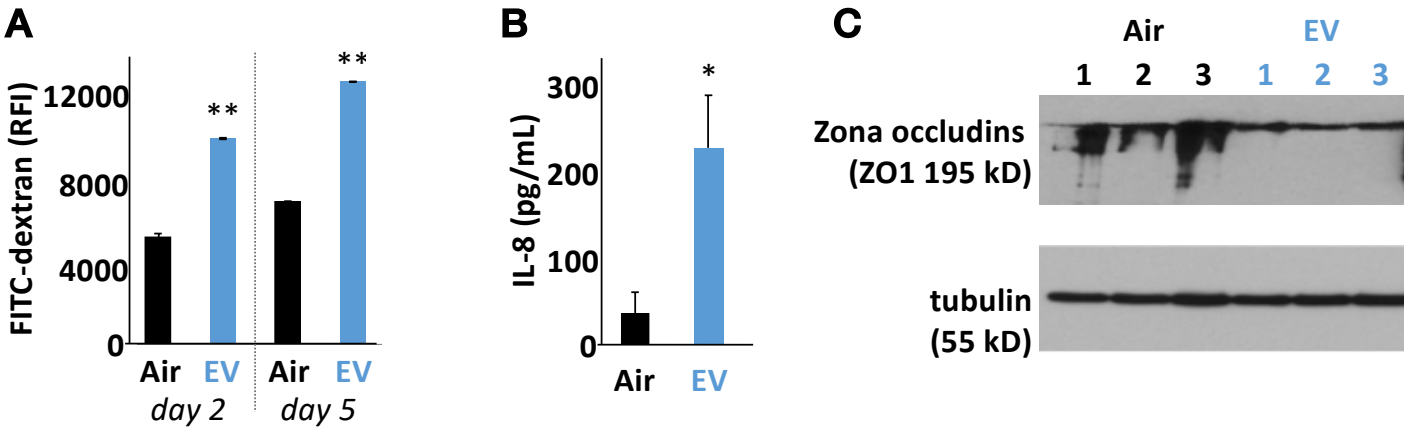

Figure 5

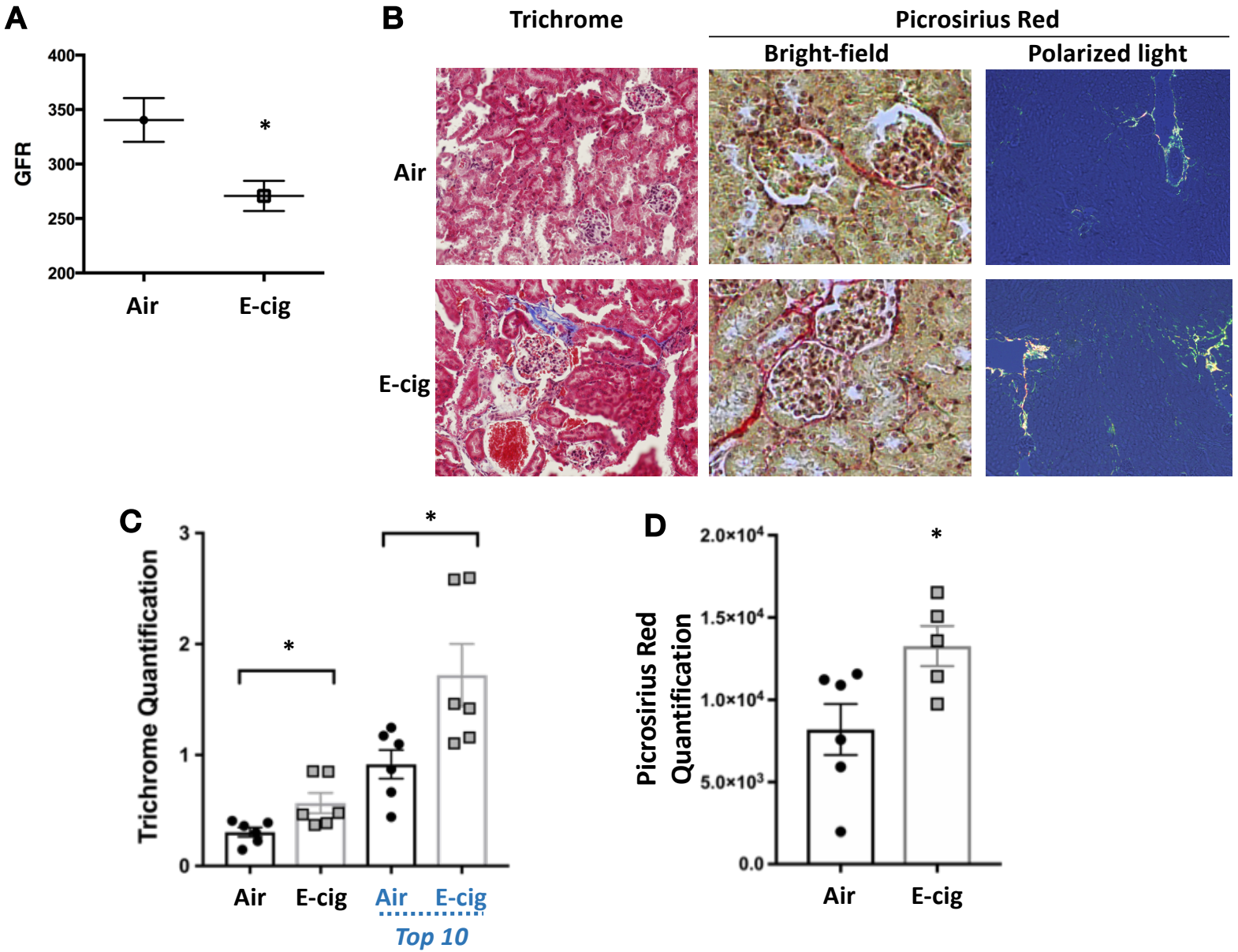

Figure 6

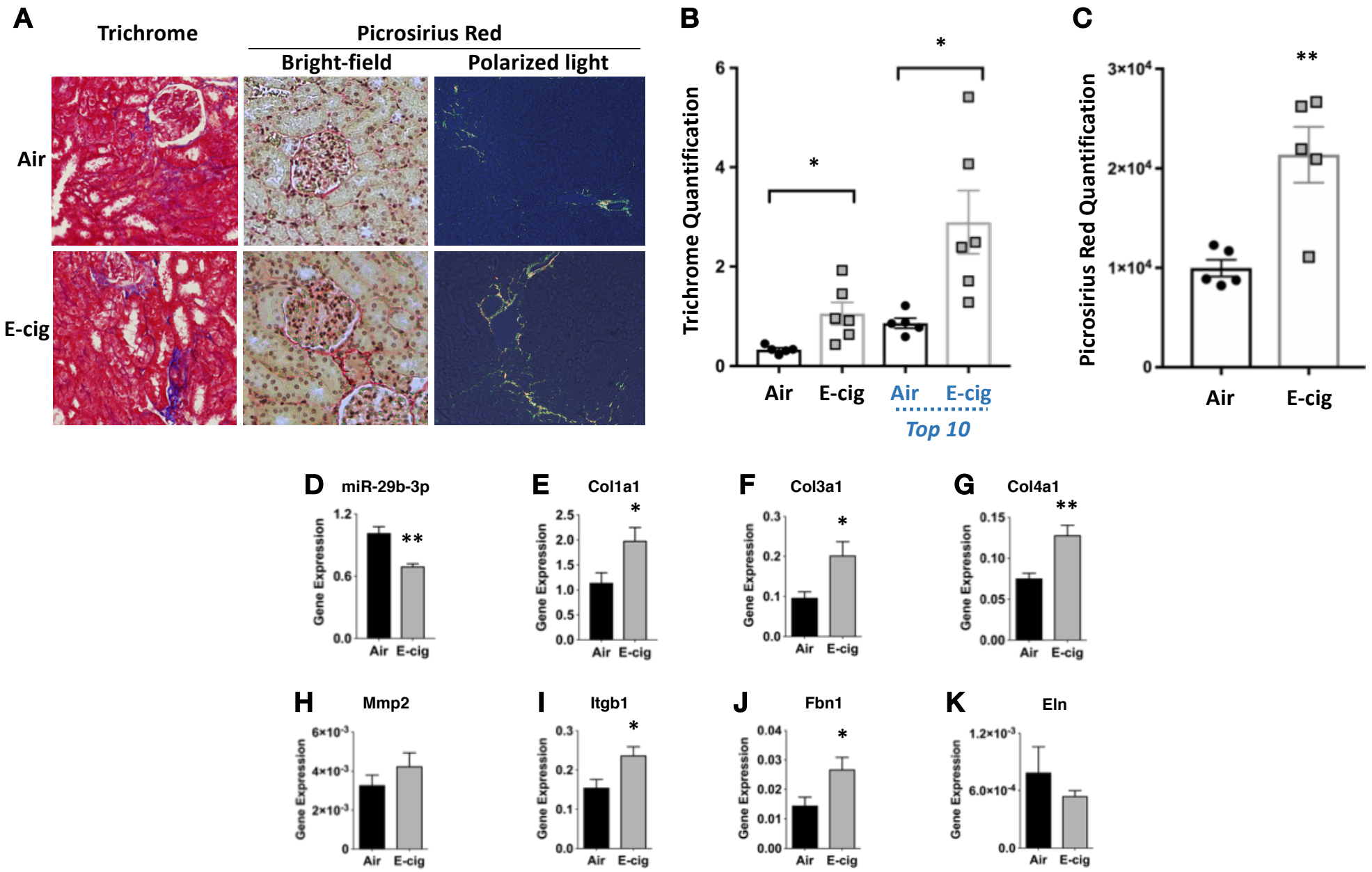

Figure 7

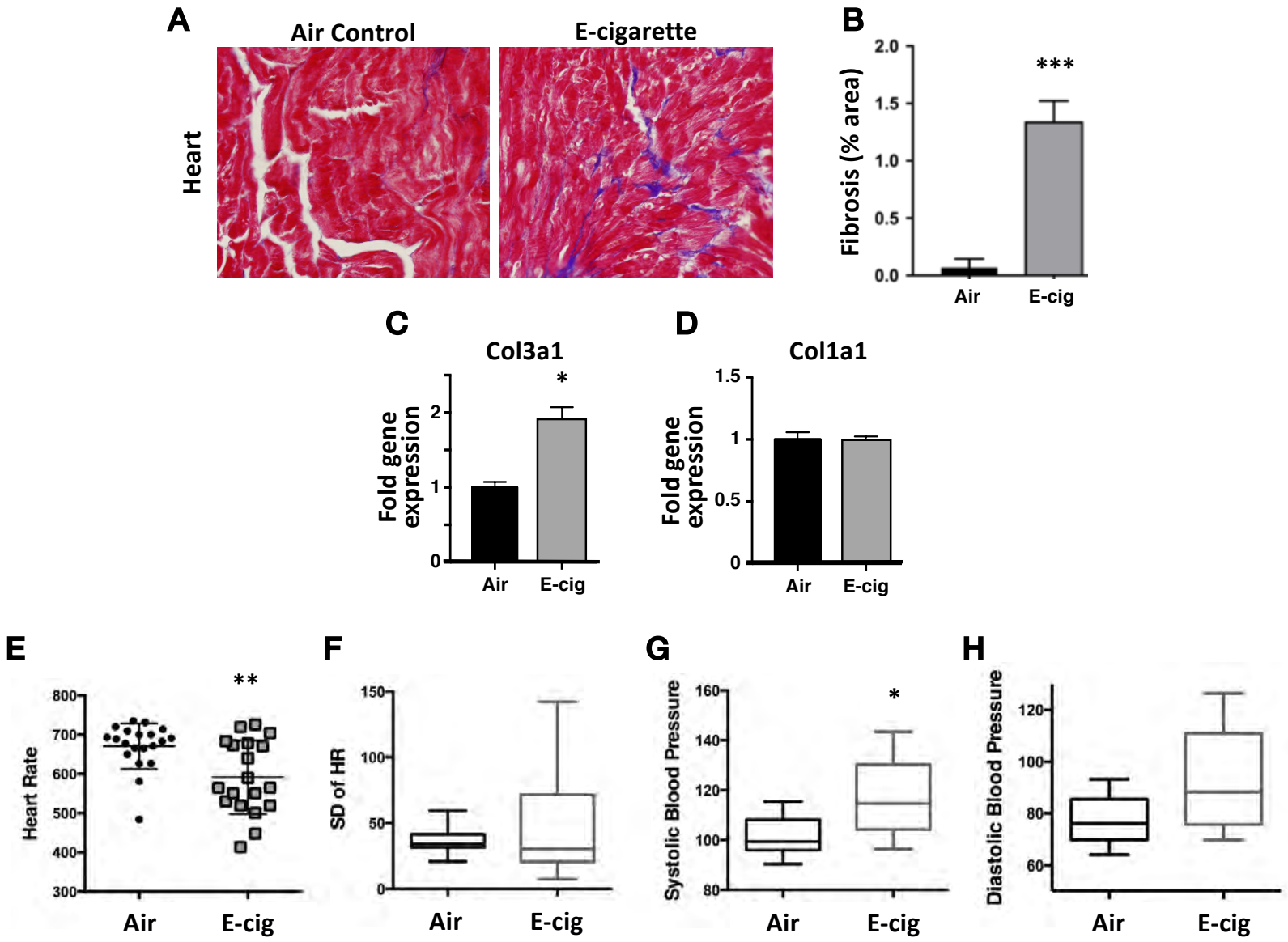

Figure 8